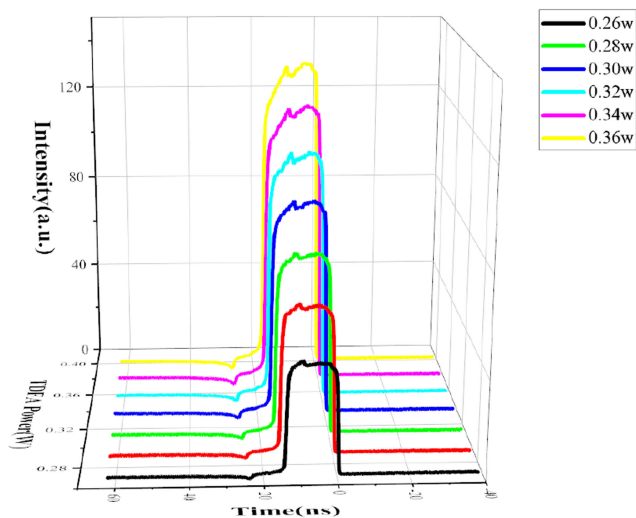


# Square-Wave Pulse Passively Mode-Locked Thulium-Doped Fiber Laser With Adjustable Pulse Duration and Amplitude

Volume 13, Number 3, June 2021

Yijuan Jiang  
Simin Liu  
Zuxing Zhang



DOI: 10.1109/JPHOT.2021.3081711

# Square-Wave Pulse Passively Mode-Locked Thulium-Doped Fiber Laser With Adjustable Pulse Duration and Amplitude

Yijuan Jiang, Simin Liu, and Zuxing Zhang 

Advanced Photonic Technology Lab, College of Electronic and Optical Engineering, Nanjing University of Posts and Telecommunications, Nanjing 210023, China

DOI:10.1109/JPHOT.2021.3081711

This work is licensed under a Creative Commons Attribution 4.0 License. For more information, see <https://creativecommons.org/licenses/by/4.0/>

Manuscript received April 4, 2021; revised May 13, 2021; accepted May 15, 2021. Date of publication May 19, 2021; date of current version June 8, 2021. This work was supported from the National Natural Science Foundation of China under Grant 91950105, and 1311 Talent Plan of Nanjing University of Posts and Telecommunications. Corresponding author: Zuxing Zhang (e-mail: zxzhang@njupt.edu.cn).

**Abstract:** A passively mode-locked thulium-doped fiber laser with square-wave pulse generation has been demonstrated using a figure-of-eight configuration with two gain mediums respectively located in the left and right loops. In this laser, mode-locking is achieved based on equivalent saturation absorption of a nonlinear amplifying loop mirror (NALM). The pulse amplitude and width of the square-wave pulse can be continuously extended through controlling pump power of gain mediums in the left and right loops. Moreover, the pulse dynamics and autocorrelation trace reveal the obtained square-wave pulse is a new kind of noise-like pulse, i.e., noise-like square-wave pulse, with capability of supporting higher pulse energy. This find enriches laser pulse dynamics and has important potential applications in laser detection, sensing and other fields.

**Index Terms:** Square-wave pulse, noise-like pulse, thulium-doped fiber laser, mode-locked laser.

## 1. Introduction

In recent years, thulium-doped fiber laser operating in the around  $2 \mu\text{m}$  “eyesafe” spectral region, has become one of research hotspots in the field of laser, due to its important application prospects in medicine, material processing, optical communication, optical fiber sensing, remote sensing and radar technology [1]. Especially about the passively mode-locked thulium-doped fiber laser for ultrashort pulse generation, a variety of research results have been reported [2], [3]. Generally, like fiber lasers at  $1.5 \mu\text{m}$  and  $1 \mu\text{m}$ , mode-locking techniques, such as semiconductor saturable absorber (SESAM) [4] or other saturable absorber material [5], [6], nonlinear polarization rotation (NPR) [7], [8], nonlinear optical loop mirror (NOLM) [9], and nonlinear amplifier loop mirror (NALM) [10], [11], have all been used to achieve passively mode-locking in thulium-doped fiber lasers. Among these, NOLM/NALM may lead to improved stability and robustness, particularly when an all-polarization-maintaining configuration is adopted [12].

Depending on cavity dispersion and nonlinearity, mode-locked fiber lasers, as an excellent research platform of soliton pulse dynamics, offer versatile pulse operation regimes, such as

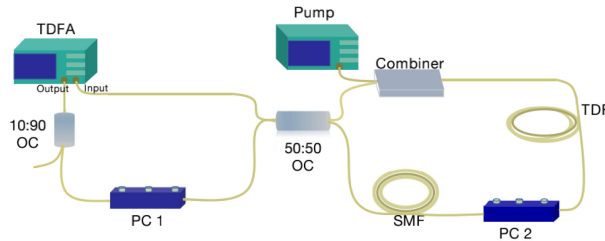


Fig. 1. Experimental setup of our proposed square-wave pulse thulium-doped fiber laser with tunable width and amplitude.

conventional soliton [13], dissipative soliton [14], [15], self-similar pulse [16], dissipative soliton resonance (DSR) [17], and noise-like pulse (NLP) [18], and so on. Recently, square-wave pulse (SWP) (also called rectangular pulse), emitted from passively mode-locked fiber lasers and considered as an efficient way to immensely increase pulse energy without pulse-breaking, has attracted much attention, due to its special shape and high-energy characteristics [19], [20]. A record SWP energy of  $10 \mu\text{J}$  has been reached in a dual amplifier double-clad Er:Yb mode-locked fiber laser [21]. Moreover, there are two main operation regimes for SWP generation from fiber lasers: DSR and NLP. DSR rectangular pulse features indefinitely broaden pulse width and constant pulse amplitude with the rising pump power. Although the generation of DSR has been reported in both normal [22], [23] and anomalous dispersion regimes [24]–[26], strict resonant condition has to be met, which make it difficult to be attained. NLP is a well-known phenomenon in mode-locked fiber lasers. NLP is a wave packet consisting of many ultrashort subpulses, demonstrating an autocorrelation with narrow coherent peak situated over wide shoulder. Li *et al* obtained noisy-pulse output at  $2 \mu\text{m}$  wavelength band from an all-fiber NOLM-based passively mode-locked thulium-doped oscillator [27]. From a thulium-doped fiber laser based on the NPR technique, He *et al* experimentally demonstrated the generation of NLP with pulse energy of  $17.3 \text{ nJ}$  and spectral bandwidth of  $60.2 \text{ nm}$  obtaining [28]. From mode-locked thulium-doped fiber lasers using NALM for mode locking, Michalska *et al* reported NLP generation with spectral width of  $32.6 \text{ nm}$  [29], while Wang *et al* obtained square-wave NLPs with pulse width increased from  $0.75$  to  $1.3 \text{ ns}$  [30]. Similar with DSR, rectangular NLP sustained by high nonlinearity exhibits broaden pulse duration with increasing pump power. Recently, Deng *et al* realized a rectangular NLP centered at  $1530.5 \text{ nm}$ , but the rectangular profile gradually decayed to a Gaussian-like shape with increasing pump power [31]. Therefore, it is worth exploring whether the rectangular NLP could always maintain its shape as the raise of the pump. Also, all the reported square-wave pulses present almost unchanged or even reduced peak power with pump power increase. Rectangular pulses with adjustable peak power would be very useful for further enhancing pulse energy and practical applications.

In this paper, we presented the generation of noise-like SWP with adjustable pulse duration and amplitude from a passively mode-locked thulium-doped fiber laser with figure-of-eight configuration. The laser mode-locking is achieved based on equivalent saturation absorption of the NALM. The width and amplitude of the SWP can be independently and continuously extended, while the rectangle profile is maintained. This noise-like rectangle pulse free of peak power clamping effect has the potential to support higher pulse energy, which enriches laser pulse dynamics and has important potential applications in the laser detection, sensing and other fields.

## 2. Experiments and Discusses

The schematic of our experimental setup for SWP thulium-doped passively mode-locked fiber laser is shown in Fig. 1. The figure-of-eight configuration consists of two loops: left unidirectional and right bidirectional loops. The left unidirectional part is constructed, in turn, a thulium-doped fiber amplifier (TDFA) with maximum output power of  $2 \text{ W}$ , a  $90:10$  fiber coupler and a polarization controller (PC). The used TDFA is commercial product, in which an isolator is integrated to ensure unidirectional

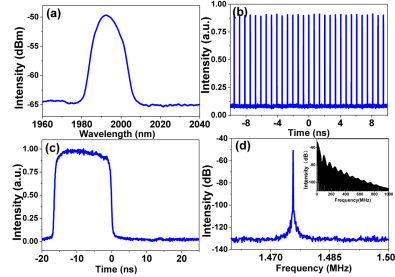


Fig. 2. Output characteristics of width and amplitude tunable square-wave pulse thulium-doped fiber laser with central wavelengths of 1992.7 nm: (a) optical spectrum, (b) pulse train, (c) single pulse profile, (b) RF spectrum.

operation. The coupler is to extract 10% energy out of the cavity and remain 90% energy in the cavity. The right bidirectional loop can be considered as a well-known nonlinear amplifying loop mirror (NALM), which can function as a nonlinear power switching device for mode locking due to the asymmetric nonlinear phase shift. The NALM is composed of a pump/signal combiner, 3.1-m long thulium-doped fiber (SM-TDF-10P130-HE), a PC and 75-m long single-mode fiber (SMF-28e). Pump light from a 793-nm laser diode with maximum pump power of 10 W is delivered to the TDF via combiner, acting as bidirectional optical amplification. The SMF is used to increase the asymmetric nonlinear phase shift between clockwise and counterclockwise propagating light in the NALM. The two loops are connected with a  $2 \times 2$  50:50 fiber coupler. Two polarization controllers (PCs) in two loops are employed to adjust the polarization state of the lasing light and optimize the birefringence to start the mode-locking. The total cavity length is 139.8 m. The light from the left unidirectional operation will be divided into two beams with equal intensity through the 3-dB coupler. The clockwise propagating beam pass the pumped TDF and SMF by turn, while for counterclockwise propagating beam the order is reversed. Owing to the asymmetric placement, there is an asymmetric nonlinear phase shift between clockwise and counterclockwise propagating light. The two beams recombine coherently at the 3-dB coupler, leading to a nonlinear transmittance at the output port of the NALM. As a result, the generation of mode-locked pulse takes place.

In the experiment, output port of the fiber coupler is connected to both an optical spectrum analyzer (OSA) and an 8 GHz real-time digital oscilloscope (OSC) with a 12 GHz optoelectronic detection module to monitor output laser spectrum and pulse train simultaneously. The laser is working in single-wavelength continuous wave state under the condition of low pump power. By increasing the pump power of the TDFA and right pump, the stable mode-locking can be obtained through adjusting the PCs. Fig. 2 shows the typical square-wave pulse emission of the laser with the TDFA pump power setting at 0.3 W and the right pump power at 6 W. Fig. 2(a) shows the pulse spectrum of the passively mode-locked thulium-doped fiber laser in the mode-locked state. The central wavelength is at 1992.7 nm and the 3-dB spectral bandwidth is 11.4 nm. The corresponding pulse train is shown in Fig. 2(b). The pulse period is 675.6 ns, corresponding to the fundamental repetition rate of 1.48 MHz. From single pulse profile of Fig. 2(c), it can be seen that the obtained pulse has a flat top with pulse duration of 16.3 ns. The RF spectrum measured by the radio frequency spectrum analyzer is shown in Fig. 2(d). The resolution bandwidth (RBW) of the RF spectrum analyzer is 50 Hz. It shows the repetition frequency of the pulse train is 1.48 MHz, corresponding to the cavity length of 139.8 m. And signal-to-noise ratio (SNR) exceeds 55 dB with a spectrum range of 450 KHz and it demonstrates that the fiber laser working in a stable mode-locked state.

Next, the relationship between square-wave pulse and TDFA pump power was investigated. First of all, we changed the pump power of the TDFA while keeping the power pump in right loop fixed at a constant power of 6 W, once square-wave pulse was achieved. Fig. 3 shows the evolution of the square-wave pulse waveform with the increased TDFA pump power from 0.26 W to 0.36 W. It can be seen that the pulse amplitude increase monotonically, but the pulse profile and duration of the output pulse remains essentially unchanged. Considering the output power, the laser fundamental

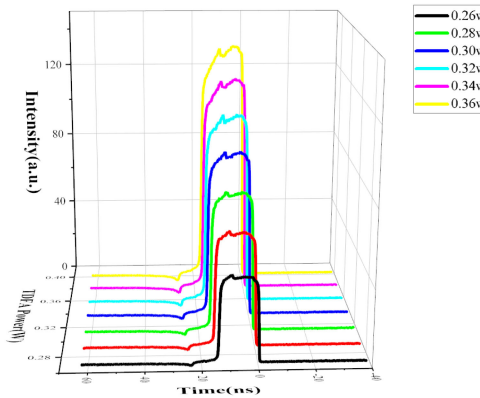


Fig. 3. Square-wave pulse evolution with the pump power of the TDFA increasing from 0.26 W to 0.36 W, when right pump power in right loop set at 6 W.

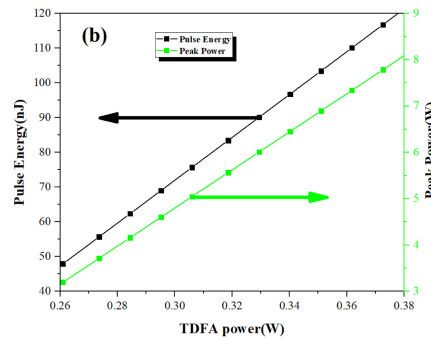


Fig. 4. Pulse energy and peak power versus TDFA pump power, when right pump power in right loop set at 6 W.

repeat rate, and the pulse width, we can calculate that the pulse energy is increasing gradually from 55.7 nJ to 116.7 nJ while peak power from 3.5 W to 7.3 W. The results are shown in Fig. 4. The pulse energy and peak power varies linearly with the pump power of TDFA. This can be understood from the laser configuration and mode-locking mechanism. The mode-locking mechanism of NALM is the asymmetric nonlinear phase shift between the clockwise and counterclockwise propagating beams, which depends on the input power and gain difference of opposite beams in the NALM. Since a 3 dB coupler was used, the power increase in the left unidirectional loop will bring about simultaneous power increase of opposite beams and has no effect on the nonlinear transmittance of the NALM. Thus, the TDFA in left unidirectional loop has only role on the pulse amplitude and energy.

Then, the relationship between square-wave pulse and pump power in right loop was explored. With the TDFA pump power in left loop setting at 0.28 W, we increased the pump power in right loop from 4 W to 10 W and recorded the single pulse waveform, as the results are shown in Fig. 5. It is noted that the state of the two PCs does not change during the process of increasing pump power. It can be seen that with the increase of the pump power, the pulses keep in the square-wave temporal profile and the width of the square pulses is broadened from 15.1 to 41.6 ns. When the pump power is 5, 6, 7, 8, 9 and 10 W respectively, the corresponding pulse duration is 15.1, 20.3, 26.1, 31.2, 37.3 and 41.6 ns, which is also recorded in Fig. 5. Meanwhile, the pulse energy can be derived from the output power and the fundamental repetition frequency as shown in Fig. 5. The pulse energy shows a linear trend with the increase of pump power from 54.5 to 125.4 nJ. But it is distinct that the peak power decreases significantly with the increase of pump power, which is completely different from the peak power clamp effect of dissipative soliton resonance [32].

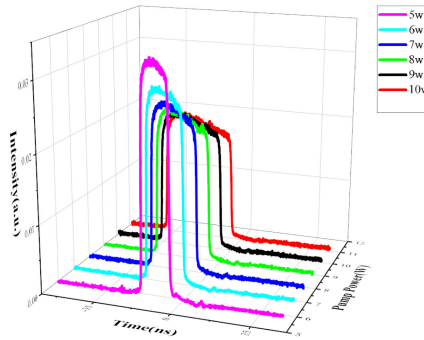


Fig. 5. Square-wave pulse evolution with the right pump power increasing from 5 W to 10 W, when TDFA pump power is set at 0.28 W.

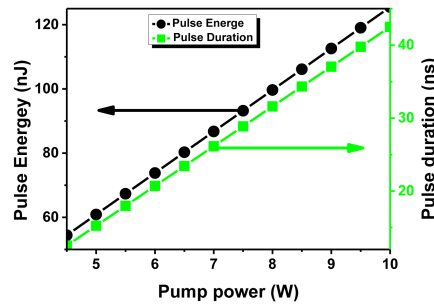


Fig. 6. Pulse energy and duration versus pump power in right loop, when TDFA pump power in left loop is set at 0.28 W.

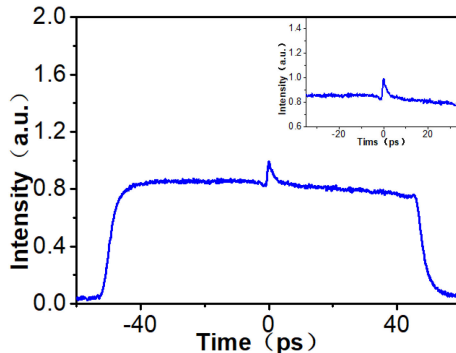


Fig. 7. The measured autocorrelation trace (the inset shows the coherent peak).

In order to investigate what kind of pulse the generated square-wave pulse is, we used an autocorrelator (FR-103XL/IR/FA) to measure the autocorrelation trace of the rectangle pulse. The results are shown in Fig. 7. It can be seen from Fig. 7 that the autocorrelation trace shows the coherent peak of narrow line width on a wide base, which is typical characteristics of noise-like pulse [33]. For clarity, we also show the coherent peak with a small scan range in the inset. The coherent peak is originated from random ultrashort subpulses due to the pulse splitting, which bunch tightly as a whole through the nonlinear interactions among each other. The noise-like pulse could tolerate the overdriven nonlinearity and broaden its duration without pulse splitting. By contrast, the DSR is actually a single pulse with peak-power clamping effect, i.e., the DSR pulse increases its width with increasing pump power while keeping the amplitude constant.

In addition, we believe that the peak power decrease with the increase of pump power is an inherent characteristic of the noise-like rectangle pulse from figure-of-eight fiber laser with two gain

mediums. In this case the peak power clamp effect is not applicable, as the peak power of the rectangle pulse can be further enhanced with the increase of the gain in unidirectional loop. The pulse energy achieved from our system can be further elevated by increasing the pump current of the left TDFA. Therefore, the results also suggest that noise-like rectangular pulse may also support higher energy as DSR, providing a new guideline for clarifying the formation mechanism of high energy rectangular pulses in fiber lasers.

### 3. Conclusion

We have demonstrated a SWP passively mode-locked thulium-doped fiber laser by using a nonlinear amplifying loop mirror (NALM). In the laser, mode-locking is achieved based on equivalent saturation absorption of the NALM. And through controlling pump power of gain mediums in the left and right loops, the pulse amplitude and width of the square-wave pulse (SWP) can be adjusted independently and continuously. Revealed by the pulse dynamics and autocorrelation trace, the obtained square-wave pulse is a new kind of noise-like pulse, with capability of supporting higher pulse energy. The passive mode-locked SWP fiber laser has important potential applications in the laser detection, sensing and other fields. It also enriches laser pulse dynamics.

---

### References

- [1] C. W. Rudy, M. J. F. Digonnet, and R. L. Byer, "Advances in 2- $\mu\text{m}$  Tm-doped mode-locked fiber lasers," *Opt. Fiber Technol.*, vol. 20, no. 6, pp. 642–649, 2014.
- [2] Z. Yan *et al.*, "Widely tunable Tm-doped mode-locked all-fiber laser," *Sci. Rep.*, vol. 6, pp. 27245, 2016.
- [3] B. Sun, J. Luo, B. P. Ng, and X. Yu, "Dispersion-compensation-free femtosecond Tm-doped all-fiber laser with a 248 MHz repetition rate," *Opt. Lett.*, vol. 41, no. 17, pp. 4052–4054, 2016.
- [4] Q. Wang, J. Geng, T. Luo, and S. Jiang, "Mode-locked 2  $\mu\text{m}$  laser with highly thulium-doped silicate fiber," *Opt. Lett.*, vol. 34, no. 23, pp. 3616–3618, 2009.
- [5] W. Zhou, D. Shen, Y. Wang, H. Ma, and F. Wang, "A stable polarization switching laser from a bidirectional passively mode-locked thulium-doped fiber oscillator," *Opt. Exp.*, vol. 21, pp. 8945–8952, 2013.
- [6] Y. Meng, Y. Li, Y. Xu, and F. Wang, "Carbon nanotube mode-locked thulium fiber laser with 200 nm tuning range," *Sci. Rep.*, vol. 7, 2017, Art. no. 45109.
- [7] X. Wang, P. Zhou, X. Wang, H. Xiao, and Z. Liu, "Pulse bundles and passive harmonic mode-locked pulses in Tm-doped fiber laser based on nonlinear polarization rotation," *Opt. Exp.*, vol. 22, no. 5, pp. 6147–6153, 2014.
- [8] P. Wang, C. Bao, B. Fu, X. Xiao, P. Grelu, and C. Yang, "Generation of wavelength-tunable soliton molecules in a 2- $\mu\text{m}$  ultrafast all-fiber laser based on nonlinear polarization evolution," *Opt. Lett.*, vol. 41, no. 10, pp. 2254–2257, 2016.
- [9] P. Honzatko, Y. Baravets, and F. Todorov, "A mode-locked thulium-doped fiber laser based on a nonlinear loop mirror," *Laser Phys. Lett.*, vol. 10, no. 7, 2013, Art. no. 075103.
- [10] M. A. Chernysheva, A. A. Krylov, P. G. Kryukov, and E. M. Dianov, "Nonlinear amplifying loop-mirror-based mode-locked thulium-doped fiber laser," *IEEE Photon. Technol. Lett.*, vol. 24, no. 14, pp. 1254–1256, Jul. 2012.
- [11] S. Smirnov, S. Kobtsev, A. Ivanenko, A. Kokhanovskiy, A. Kemmer, and M. Gervaziev, "Layout of NALM fiber laser with adjustable peak power of generated pulses," *Opt. Lett.*, vol. 42, no. 9, pp. 1732–1735, 2017.
- [12] C. Radzewicz, J. Szczepanek, M. Michalska, T. M. Kardaś, and Y. Stepanenko, "Simple all-PM-fiber laser mode-locked with a nonlinear loop mirror," *Opt. Lett.*, vol. 40, no. 15, pp. 3500–3503, 2015.
- [13] Y. Wang, S. U. Alam, E. D. Obratzsova, A. S. Pozharov, S. Y. Set, and S. Yamashita, "Generation of stretched pulses and dissipative solitons at 2  $\mu\text{m}$  from an all-fiber mode-locked laser using carbon nanotube saturable absorbers," *Opt. Lett.*, vol. 41, no. 16, pp. 3864–3867, 2016.
- [14] P. Wang, X. Xiao, and C. Yang, "Quantized pulse separations of phase-locked soliton molecules in a dispersion-managed mode-locked tm fiber laser at 2- $\mu\text{m}$ ," *Opt. Lett.*, vol. 42, no. 1, pp. 29–32, 2017.
- [15] X. Liu *et al.*, "Multistability evolution and hysteresis phenomena of dissipative solitons in a passively mode-locked fiber laser with large normal cavity dispersion," *Opt. Exp.*, vol. 10, no. 17, pp. 8506–8512, 2009.
- [16] Z. Zhang, B. Öktem, and F. İlday, "All-fiber-integrated soliton–similariton laser with in-line fiber filter," *Opt. Lett.*, vol. 37, no. 17, pp. 3489–3491, 2012.
- [17] P. Wang, K. Zhao, X. Xiao, and C. Yang, "Pulse dynamics of dual-wavelength dissipative soliton resonances and domain wall solitons in a tm fiber laser with fiber-based lyot filter," *Opt. Exp.*, vol. 24, no. 25, pp. 30708–30719, 2017.
- [18] S. Liu, F. Yan, L. Zhang, W. Han, Z. Bai, and H. Zhou, "Noise-like femtosecond pulse in passively mode-locked Tm-doped NALM-based oscillator with small net anomalous dispersion," *J. Opt.*, vol. 18, no. 1, 2016, Art. no. 015508.
- [19] N. Akhmediev, J. M. Soto-Crespo, and P. Grelu, "Roadmap to ultra-short record high-energy pulses out of laser oscillators," *Phys. Lett. A*, vol. 372, no. 17, pp. 3124–3128, 2008.
- [20] P. Grelu, W. Chang, A. Ankiewicz, J. M. Soto-Crespo, and N. Akhmediev, "Dissipative soliton resonance as a guideline for high-energy pulse laser oscillators," *J. Opt. Soc. Amer., B*, vol. 27, no. 11, pp. 2336–2341, 2010.

- [21] G. Semaan, F. B. Braham, J. Fourmont, M. Salhi, F. Bahloul, and F. Sanchez, "10  $\mu\text{J}$  dissipative soliton resonance square pulse in a dual amplifier figure-of-eight double-clad er:Yb mode-locked fiber laser," *Opt. Lett.*, vol. 41, no. 20, pp. 4767–4770, 2016.
- [22] D. J. Li, D. Y. Tang, L. M. Zhao, and D. Y. Shen, "Mechanism of dissipative-soliton-resonance generation in passively mode-locked all-normal-dispersion fiber laser," *J. Lightw. Technol.*, vol. 33, no. 18, pp. 3781–3787, 2015.
- [23] X. Wu, D. Y. Tang, and H. Zhang, "Dissipative soliton resonance in an all-normal dispersion erbium-doped fiber laser," *Opt. Exp.*, vol. 24, no. 9, pp. 9966–9974, 2016.
- [24] W. Chang, J. M. Soto-Crespo, A. Ankiewicz, and N. Akhmediev, "Dissipative soliton resonances in the anomalous dispersion regime," *Phys. Rev. A*, vol. 79, no. 3, 2009.
- [25] I. Armas-Rivera *et al.*, "Dissipative soliton resonance in a full polarization-maintaining fiber ring laser at different values of dispersion," *Opt. Exp.*, vol. 7, no. 17, pp. 5580–5584, 2009.
- [26] F. B. Braham, G. Semaan, F. Bahloul, M. Salhi, and F. Sanchez, "Experimental optimization of dissipative soliton resonance square pulses in all anomalous passively mode-locked fiber laser," *J. Opt.*, vol. 19, no. 10, 2017, Art. no. 105501.
- [27] J. Li *et al.*, "All-fiber passively mode-locked Tm-doped NOLM-based oscillator operating at 2- $\mu\text{m}$  in both soliton and noisy-pulse regimes," *Opt. Exp.*, vol. 22, no. 7, pp. 7875–7882, 2014.
- [28] X. He *et al.*, "60 nm bandwidth, 17 nJ noiselike pulse generation from a thulium-doped fiber ring laser," *Appl. Phys. Exp.*, vol. 6, no. 11, 2013, Art. no. 112702.
- [29] M. Michalska, and J. Swiderski, "Noise-like pulse generation using polarization maintaining mode-locked thulium-doped fiber laser with nonlinear amplifying loop mirror," *IEEE Photon. J.*, vol. 11, no. 6, Dec. 2019, Art. no. 1504710.
- [30] T. Wang, W. Ma, Q. Jia, Q. Su, P. Liu, and P. Zhang, "Passively mode-locked fiber lasers based on nonlinearity at 2  $\mu\text{m}$  band," *IEEE J. Sel. Topics Quantum Electron.*, vol. 24, no. 11, May/Jun. 2018, Art. no. 1102011.
- [31] Z. Deng *et al.*, "Switchable generation of rectangular noise-like pulse and dissipative soliton resonance in a fiber laser," *Opt. Lett.*, vol. 42, no. 21, pp. 4517–4520, 2017.
- [32] L. Mei *et al.*, "Width and amplitude tunable square-wave pulse in dual-pump passively mode-locked fiber laser," *Opt. Lett.*, vol. 39, no. 11, pp. 3235–3237, 2014.
- [33] H. Santiago-Hernandez *et al.*, "Generation and characterization of erbium-Raman noise-like pulses from a figure-eight fibre laser," *Laser Phys.*, vol. 25, no. 4, 2052, Art. no. 045106.